PREDICTING THE DYNAMIC BEHAVIOUR OF POLYMER COMPOSITES

Lucio Raimondo*, Lorenzo Iannucci* Paul Robinson*, Silvestre T. Pinho*, Paul T. Curtis, Garry M. Wells****

***Imperial College London, Department of Aeronautics, South Kensington Campus, London SW7 2AZ **Defence Science and Technology Laboratory, Porton Down, Wiltshire SP4 0JQ**

Abstract

This paper describes experimental and numerical research activities aimed at the development, implementation into an explicit FE code, and validation of a state-of-the-art composite material model for dynamic failure. The developed material model, which can predict the behaviour of UD Carbon Fibre Reinforced Polymer (CFRP) composites, is implemented into LS-DYNA3D for solid brick elements with one integration point. Though the developed model has wide applicability, this paper focuses on aspects related to validation against composites ballistic data.

1 Introduction

The development and validation of Finite Element (FE) simulation tools can reduce costs and time within the industrial development cycle since full-scale experimental impact tests are prohibitively expensive and time consuming. This is a major concern for aircraft industries as fibre-reinforced polymer composite structures are used in safety critical primary structures, such as wing boxes, and aero-engines, such as compressor blades, where the risk of high velocity impacts (HVI) is significant due to bird-strikes or to fragments of failed turbine-engine blades. The use of composite materials in space structures is also increasing with polymer matrix composites extensively used in spacecraft structures and satellite components such as antenna struts, panels and low distortion frames, which are subjected to the threat of hypervelocity impacts from micrometeorites. Polymer composites are also being used in the production of light weight vehicles and body armour because their use reduces the costs of production and transportation. The lack of robust and detailed material models, particularly for damage propagation, restricts the optimization of a composite structure, and much research is underway in this field.

2 HVI experiments

2.1 Motivations

Coupon-scale rather than full-scale testing is typically performed in industry, as well as in research centres or universities, because of the limitations imposed by cost, time and safety. Limits also exist for the types of impact conditions that can be recreated in a laboratory. Relating the in-service impact behaviour of composite components and structures to the impact behaviour of laboratory coupons is not simple. However, detailed coupon-scale impact test data with varying impact parameters might improve confidence in the design of parts that must operate under specific operational conditions. Moreover, detailed quantitative ballistic data and a correct phenomenological interpretation of the mechanisms of fracture are essential for the development and thorough validation of numerical material models for crashworthiness applications.

Thus, the experimental work presented in this paper is motivated by two main reasons: 1) need for detailed high velocity test data for NCF composites, which are missing in the dedicated literature [1-5]; 2) need for detailed quantitative information that can support the development of advanced numerical tools for application into the HVI regime.

2.2 Materials, designation and HVI apparatus

All composite panels that were tested in this work were manufactured with bi-axial NCF carbon fibrous reinforcement and with RTM6 epoxy resin. All panels were manufactured in accordance with the optimised manufacturing process described in ref. [6]. CAI standard [7] size (SS) coupons and reduced size (RS) coupons were cut out of the panels. Only results for RS coupons are reported in

this paper. The complete series of data which was generated is available in ref. [8], which also includes ballistic tests data for glass and hybrid glass/carbon NCF/RTM6 RS coupons. The dimensions of the RS targets, with relative boundary tests conditions, are illustrated in Fig. 1.
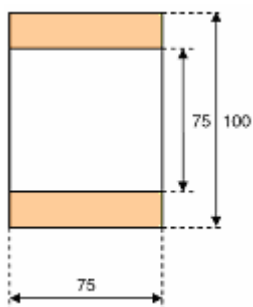

Fig. 1. RS coupons geometry and boundary conditions (shaded regions are fully clamped). Dimensions in mm.

The CF NCF used was Type 2A DB and Type 2B DB NCF purchased from Devold AMT, NO. The NCF material was Tenax 12K HTS 5631-Ae/ Carbon with polyester non-text stitch yarn of chain type, with stitch length of 2.5mm, low stitch tension, and space between stitches of 5.1mm.

In the following, the standard notation adopted for lay-ups of UD laminates is used for lay-ups with bi-axial NCF reinforcement. Both $[0/90]_{2nS}$ ("XP") and $[0/90/+45/-45]_{nS}$ ("QI") CF panels were manufactured, with $n = 2$ and $n = 4$ for panels with mean nominal thicknesses equal to 2.17mm and 4.4mm, respectively.

An instrumented single stage gas gun was used for ballistic testing, see Fig. 2.
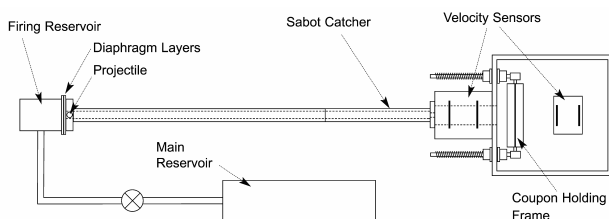

Fig. 2. Schematic representation of the gas-gun set-up

Both nitrogen and helium gases were used to propel the sabots. These accelerated 6mm diameter steel balls when no otherwise stated. Tests were also conducted using tungsten carbide and titanium balls.

The projectile velocity was recorded immediately before ("impact velocity") and after ("residual velocity") impact by means of two velocity sensors built with photodiodes sensors at a set distance.

2.3 Characterisation of impact damage

Fig. 3 shows a fibre tensile fracture pattern at 90° to the fibres direction along the axis of maximum local bending on the face of CF 2mm thick specimen impacted at its ballistic limit. Relatively long transverse matrix cracks are also evident, running on the sides of the depressed zone which are parallel to the fibre direction. The number and relatively "clean look" of the visible fibre fragments indicates that matrix cracking and crushing occurred at the impact point. A "crater", with diameter equal to the projectile's diameter, is observed in the contact region of the 4mm thick coupons impacted at velocities close to or higher than their ballistic limit. Fractured fibres and fragments of fibres are visible by naked eye within the crater, see Fig. 4.

Fig. 3. Detail of the impact point in a CF QI 2.15mm coupon impacted at 161m/s.

Fig. 4. Front face of a CF XP 4.16mm thick coupon impacted at normal incidence and at a speed of 293m/s.

It is noticeable, from analysis of the top and bottom areas of the crater zone shown in Fig. 4 and from analysis of the two misaligned bundles of fibres visible on the left-hand side of the crater, that all fibres crossing the impact region were subject to tensile failure along the axis of maximum local bending also in this thicker specimen. However, entire segments of fibres were "driven off" the impact region in 4mm thick specimens. This is probably the result of higher impact energies achieved when testing thicker specimens. The sharp fibre fracture surfaces that are visible at the left and right hand sides of the crater in Fig. 4 and in Fig. 3, indicate a shear plug failure mode, or possibly a fibre compressive failure, at the boundaries of the crater zone which are perpendicular to the fibre direction.

The extent of frontal face fibres splitting and delamination was found to increase with increasing impact velocity for 4mm thick specimens. No front face delamination and only limited fibre splitting was evident for 2mm thick samples.

Asymmetric delamination and transverse cracking patterns were visible on the front face of the specimens impacted by projectiles with a 40° incidence at ballistic velocities, see Fig. 5.

Fig. 5. Detail of the front face of a CF QI 4.16mm thick coupon impacted at 317 m/s with 40 incidence.

Severe permanent deformations are evident at the rear face of all impacted specimens. Specimens that were impacted at velocities lower than the ballistic limit show evidence of a wide delamination of the rear ply. A large number of transverse matrix cracks are visible on the outer layer, in most cases inter-bundle cracks, i.e. matrix cracks would initiate and develop within the resin rich pockets contained in the NCF bundles. Delamination of this ply is likely to occur in mode I as segments of broken fibres from the inner layers are pushed against its centre, as shown in Fig. 6. From analysis of the inner plies visible from the rear face of specimens, as shown in Fig. 6, it can be deduced that tensile fibre failure occurred along the axis of maximum local bending in all plies, and that transverse matrix

cracking occurred only within the bundles that failed in a fibre tensile mode. Also, there is no evidence of transverse inter-bundles cracks on the surface of the inner plies which are visible. Fig. 7 shows the cross-section of the specimen photographed in Fig. 4. From the analysis of this Fig. 7, there is clear evidence of fibre failure in the through-thickness direction. Also, there is evidence of matrix crushing and cracking in a volume that expands from the front face towards the rear face in a regular conical shape, as outlined by the dashed lines.

Fig. 6. Detail of the back face of a CF XP 4mm sample impacted at 295 m/s (ballistic limit) at 40° incidence.
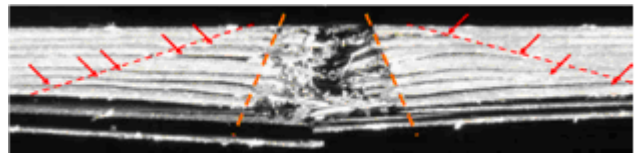

Fig. 7. Photograph of the section of a CF XP 4.16mm thick coupon impacted at normal incidence at 293 m/s, with details of through-thickness damage pattern.
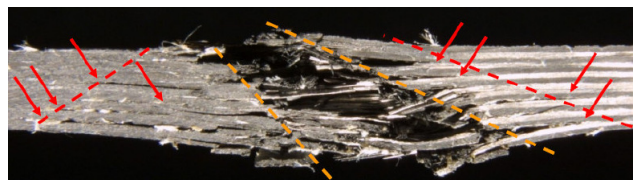

Fig. 8. Section of a 4.34 mm thick CF XP coupon impacted at 290 m/s at 40° incidence. The arrows point at interlaminar cracks tips.

Arrows are drawn which point at the tips of interlaminar cracks. Interlaminar cracks on the section imply delaminations within the specimen. Analysis of the specimens sections for impacts at 40° incidence (see Fig. 8) would indicate that the angle

of attack of the projectile did not change dramatically with penetration depth for velocities higher than the ballistic limit. Fig. 8 shows that the matrix and fibre crushed volume expands with an asymmetric conical shape from the impact point to the rear face of the specimen.

The effects of impact velocity were found to play a major role on damage propagation whether this was on the front or on the rear face, or through-thickness of the targets. For instance, delaminations areas (detailed C-Scan data from the tests is available in ref. [8]) were found to be a function of the impact energy and velocity. This is fundamentally different from what is observed for low impact velocities, for which damage propagates only as function of impact energy and is independent of impact velocity. The high velocity impact regime could be defined as that in which damage propagation would be a function of impact energy as well as of impact velocity. This qualitative definition translates into the mathematical model proposed in ref. [9] when the damage being considered is the through-the-thickness matrix crushing of the composite target.

3 UD CFRP composite material model

3.1 Introduction

Application of current visual investigation techniques gives limited information on the exact dynamics of HVI damage development. Thus, accurate prediction of the HVI behaviour of polymer composites is not trivial. The most realistic approach is based on applying failure and damage approaches validated for regimes in which the material can be characterised via of controlled tests. However, the loading conditions generated upon HVI cannot easily be reproduced by means of any other existing experimental characterisation technique. Thus, classic failure theories and damage approaches can be inaccurate when applied in this regime. Polymer composites exhibit visco-elasto-plastic behaviour and strain-rate dependent failure properties. Propagation of failure also depends on strain rate in these materials.

It is argued that constitutive modelling approaches that are based on physically sound arguments should be preferred amongst the various available approaches, especially when the application is for HVI modelling. This is because physically-based modelling approaches can succeed in simulating material failure in a loading space that extends beyond the space of characterisation of the material parameters.

A series of modelling strategies have been proposed for predicting composite impact damage within the low and medium velocity regime. In [10] it was pointed out that there are four main different strategies that have been employed: 1) a failure criteria approach; 2) a fracture mechanics approach; 3) a plasticity or yield surface approach; 4) a damage mechanics approach. Published works were found in the open literature on composites HVI modelling [11-14]. The approaches typically fall in one or more of the categories listed above, but it is apparent that no works published in the literature used phenomenological based failure approaches. "Hybrid approaches" can be particularly effective. An attractive failure and damage modelling strategy was proposed in ref. [15] based on the combined application of the strategies 1), 2) and 4) that were listed above: phenomenological failure criteria were applied to predict damage initiation, a Continuous Damage Mechanics (CDM) approach based on fracture mechanics was applied for predicting damage evolution. Such hybrid techniques proved to be accurate in predicting the low-velocity impact response of polymer composites [16].

3.2 Proposed modeling strategy

The proposed UD HVI material model is based on the combined application of plasticity, failure, damage mechanics and fracture mechanics. The developed model is an "enhanced" version of a failure and damage model previously implemented in LS-DYNA3D [17]. Further background information is available in ref. [15, 18], as in this paper only further modelling developments are discussed.

The material model here developed can be defined as Strain-Rate dependent (plus) Damage (plus) Energy-Based composites failure material model. This model predicts strain-rate-dependent non-linear material behaviour. Geometric non-linearity is also modelled by means of damage variables defined according to the classic DM approach. The damage evolution laws are defined as a function of the energy release rates for the specific failure modes and a characteristic element length is used to scale the fracture energy with element size. Thus the results are independent of mesh size. Strain-rate dependent damage evolution laws are also modelled. Damage initiation thresholds are predicted by application of dynamic failure criteria for the matrix (tensile and compressive) and the pure

shear failure modes, and static failure criteria for the fibre tensile and compressive failure modes.

The following convention is adopted in the next of this paper: a material reference frame is defined in the (abc) space. The axis (a) has the direction of the fibers in a UD lamina. The axis (b) has the direction perpendicular to direction (a) and lies in the plane of the lamina. The reference axis (c) completes the orthogonal axes with the (a) and the (b) axes.

3.3 3D strain-rate dependent plasticity theory

The 3D strain-rate dependent plasticity theory, which is applied in the present work, has been derived, implemented into FE and validated in ref. [19]. It is applicable for predicting strain-rate dependent non-linear behavior of UD composites with polymer matrix. The theory is physically-based and it was developed based on extending the applicability of the Mohr-Coulomb criterion for matrix compressive failure. Non-linearities and strain-rate sensitivity of matrix dominated mechanical properties were assumed to result from inelastic shear effects in a reference frame which is rotated with respect to the principal material symmetry frame. The frame in which strain-rate dependent plasticity can be modeled was assumed in [19] to be aligned with the potential matrix fracture plane [15]. Because non-linear shear stress-strain functions are used for modelling material non-linearity in the generic loading case, the non-linear shear stress-strain curves in the (ab), (bc) and (ac) planes are required by the model. The shear plasticity model, which is described in details in ref. [19], can predict unloading paths from an arbitrary state assuming no hysteresis but shear stiffness reduction with strain, see Fig. 9. Strain-rate sensitivity was added [19] for the pure shear behaviour by using a scaling function, whose coefficients can be determined from analysis of dynamic and quasi-static pure shear stress-strain data. Fig. 10 shows how accurate a model, which uses scaling functions is in predicting the composite shear behaviour at different strain rates.

When modelling non-linear strain-rate dependent shear behaviour in the reference frame aligned with the potential fracture plane, non-linear and strain-rate dependent response is predicted for deformations along all directions affected by the matrix behaviour, i.e. pure shear response in planes (ab), (bc) and (ca), and response along principal directions (b) and (c).
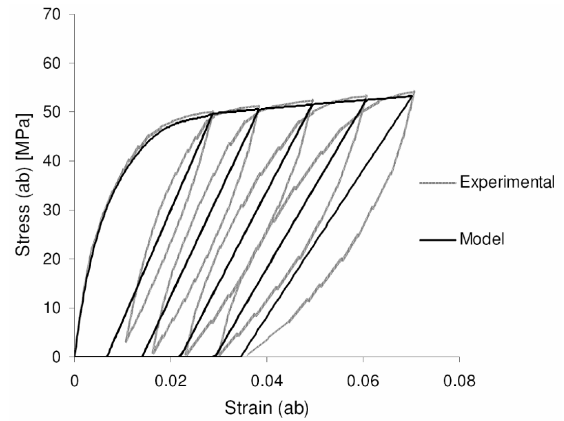

Fig. 9. Shear model [19] prediction vs. experimental results, these are from ref. [20].
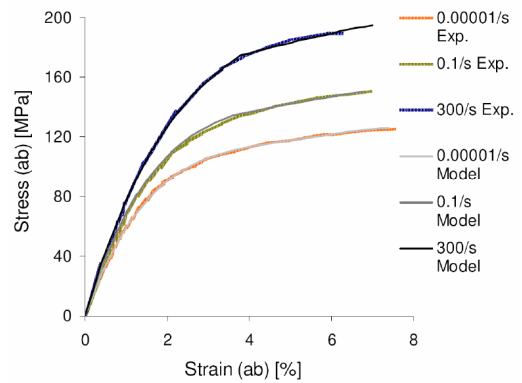

Fig. 10. Shear stress-strain curves under quasi-static and high strain rate loading. Experimental results from ref. [21].
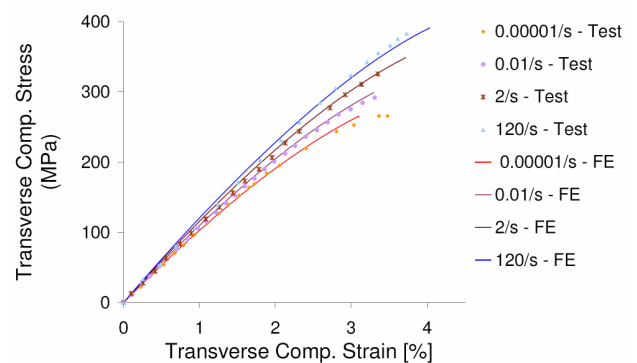

Fig. 11. Transverse compressive stress-strain numerical and experimental curves for varying strain-rates.

For instance, Fig. 11 shows that very good predictions of material behaviour in direction (b) can be achieved by applying the recently developed [19] strain-rate dependent 3D plasticity theory. In this

Fig. 11 experimental and numerical transverse compressive stress-strain curves are plotted for a UD IM6G/3501-6 carbon/epoxy composite under quasi-static and dynamic loading (the experimental results were available in the literature and are from ref. [21].

3.4 The failure criteria

3.4.1 Fibre tensile failure

For fibre failure the maximum stress criterion is used:

$$f_{ft} = \left(\frac{\sigma_a}{X_T}\right)^2 - 1 = 0 \qquad (1)$$

in which X_T is the tensile failure strength in the fibre direction, a.

3.4.2 Fibre Compressive failure

For fibre compression failure, the maximum stress criterion is used:

$$f_{fc} = \left(\frac{\sigma_a}{X_C}\right)^2 - 1 = 0 \qquad (2)$$

in which X_C is the compressive failure strength in the fibre direction.

3.4.3 Matrix compressive failure

For matrix compressive failure, the LaRC04 matrix compression criterion [15], is further modified including dynamic enhancement of traction strengths with traction strain-rate:

$$f_{mc} = \left(\frac{\tau_T}{S_{T,D} - \mu_T \sigma_n}\right)^2 + \left(\frac{\tau_L}{S_{L,D} - \mu_L \sigma_n}\right)^2 = 1 \qquad (3)$$

$S_{T,D}$ and $S_{L,D}$ are the dynamic traction strengths, which are defined as a function of traction strain-rate, e.g.:

$$S_{T,D} = z\left(\dot{\gamma}_{b'c'}\right) S_T \qquad (4)$$

where z is a scaling function defined as the ratio between the pure shear dynamic strength, $S_{bc,D}$, and the pure shear quasi-static strength, S_{bc}, which can be characterized experimentally. It is here assumed that the composite has same strain-rate sensitivity when deformed in transverse and longitudinal shear and that strain-rate sensitivity is material frame independent, e.g. z is used to predict both $S_{T,D}$ and $S_{L,D}$. As typically longitudinal shear high-rate data is available, z is here defined as:

$$z = \frac{S_{ab,D}}{S_{ab}} \qquad (5)$$

Fig. 12 shows predictions obtained applying the dynamic matrix compression failure criterion here proposed.
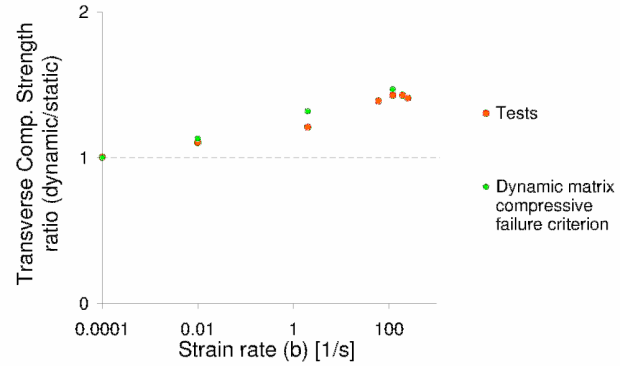

Fig. 12. Dynamic transverse compressive dynamic strength ratios for a UD IM6G/3501-6 carbon/epoxy under quasi-static and dynamic loading. Experimental results from ref.[21].

3.4.4 Matrix tensile failure

For matrix tensile failure, the criterion proposed in ref. [15], is modified to include strain rate enhancement of traction strengths:

$$f_{mt} = \left(\frac{\sigma_n}{Y_T}\right)^2 + \left(\frac{\tau_T}{S_{T,D}}\right)^2 + \left(\frac{\tau_L}{S_{L,D}}\right)^2 = 1 \qquad (6)$$

where Y_T is the matrix tensile failure strength.

3.4.5 Pure shear failure

For shear failure, the following dynamic criteria are used, e.g. for pure shear failure in the plane (ab):

$$f_{ab} = \left(\frac{\tau_{ab}}{z\left(\dot{\gamma}_{ab}\right) S_{ab}}\right)^2 - 1 = 0 \qquad (7)$$

And similar criteria are applied for predicting pure shear failure in the planes (bc) and (ac).

3.5 Strain-rate dependent energy-based CDM approach

An energy based damage formulation for modelling propagation of fractures whose initiation is predicted by the rate independent versions of the criteria was proposed and implemented in LS-DYNA3D for a composite with non-linear in-plane shear behaviour [15]. The material model here developed simulates non-linear strain-rate-dependent material behaviour in 3D. Thus, the approach described in ref. [15] has been re-formulated [19] to

account for 3D non-linear material response on the plane of fracture propagation. The damage evolution laws are rate-dependent for matrix compressive, tensile and pure shear failure. It is here assumed that a relationship of direct proportionality exists between shear traction strengths and fracture toughness. This is a simplification and dynamic fracture energies should be experimentally characterised. For the case of matrix tensile and compressive failure, a "dynamic fracture energy", $\overline{\Gamma}$, is thus used for calculation of the damage evolution laws and it is defined as follows:

$$\overline{\Gamma} = \Gamma_b \left\langle \frac{\sigma_{b'}^0}{\sigma_{mat}^0} \right\rangle^2 + z\left(\dot{\gamma}_{b'c'}\right)\Gamma_{b'c'}\left\langle \frac{\tau_{b'c'}^0}{\sigma_{mat}^0} \right\rangle^2 + ...$$

$$... z\left(\dot{\gamma}_{ab'}\right)\Gamma_{ab'}\left\langle \frac{\tau_{ab'}^0}{\sigma_{mat}^0} \right\rangle^2 \tag{8}$$

All relevant quantities in this Eq. (8) have been previously defined in this paper and in ref. [15].

3.6 Coupling of constitutive, failure and damage formulations

The coupling between the 3D strain-rate dependent plasticity theory, the dynamic failure criteria and the strain-rate dependent DM approach is illustrated in Fig.13 and Fig.14. All relevant operations are performed on the shear traction stress-strain behaviour on the fracture plane (Fig.13) and these result in 3D effects in principal material axes (Fig.14). Simple bi-linear strain-stress behaviour is assumed for both tensile and compressive response in the fibre direction (a), which is assumed strain-rate independent.
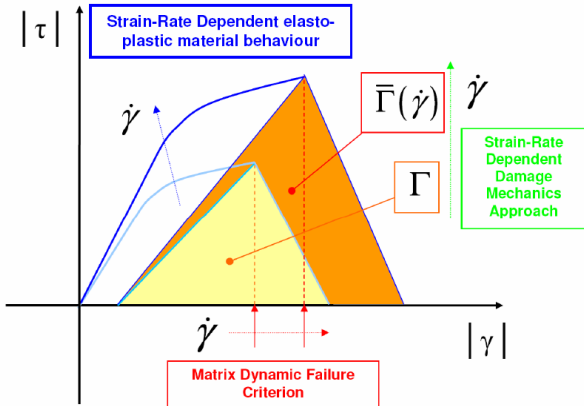

Fig.13. Modelling the local traction behaviour on the plane of progressive failure.
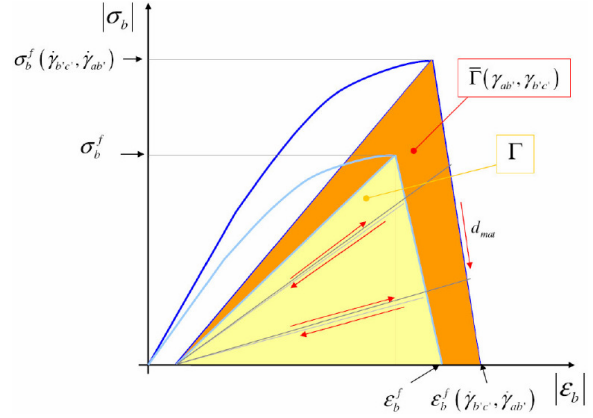

Fig.14. Resulting dynamic effects for transverse (matrix) compressive deformation.

3.7 Model validation

The experimental impact tests are simulated with the proposed model. A range of cases are investigated covering effects of thickness, lay-up, impact angle and projectile density. Fig. 15 shows a sample frame from the numerical simulation of an impact of a 6mm-diameter steel ball traveling at 440 m/s and 40° incidence onto a CF XP 4.52mm coupon (64 μs impact time). Both target and impactor are simulated using single-point integration solid elements available in LS-DYNA [22]. The impactor is simulated as a rigid body and each individual ply of the composite target is simulated using the failure and damage model which are described in the earlier paragraphs of this section.
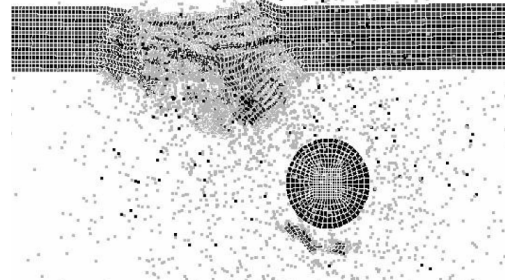

Fig. 15. Sample frame from HVI numerical simulation using the proposed model.

The definition of a strategy for elements erosion is necessary for successfully simulating ballistic penetration using Lagrangian FE approaches. Distorted elements must be eliminated for two main reasons, i.e. 1) Experimental evidence:

composite fragments are driven off the target during penetration; 2) Stability of the numerical analysis: the Lagrangian local reference frame is fixed to the base of a solid element and is oriented depending on the base nodes numbering and their relative position.

If the elements distort severely and the nodes undergo relative movement the Lagrangian approach becomes inaccurate [22]. Elements can be eroded in LS-DYNA by the definition of a user-defined criterion. The physical based failure criteria, in combination with the damage mechanics approach, which are applied in the present work, predict very specific orientations of damage initiation and propagation. This results in failing elements having load-bearing capability in all the directions that have not failed or completely failed yet. A rigorous analysis using the present formulation would require that the failing elements had dimensions comparable to the crack width. This is unreasonable as such a refined mesh would be too computationally expensive. The threshold for element erosion should thus not be based on the value of the damage variables but failed elements should be deleted if they distort too much. Thus, elements that are too distorted, rather than elements that have "failed", should be deleted from the mesh. The criterion for element erosion takes the following form:

$$f_{erosion} = \min\left(f_{ft}, \max\left(\gamma_{ab}, \gamma_{bc}, \gamma_{ac}\right) - \Omega\right) = 0$$

In which Ω is a user-defined parameter, i.e. $\Omega = 1.25$ for the current simulations.

Fig. 16, and Fig. 17, Fig. 18 and Fig. 19 show a selection of results from the impact tests and simulations using the proposed model. Very good correlation is obtained between experimental and numerical ballistic curves. The effects of lay-up were not evident from both tests and simulations for both the ~2mm and ~4mm thick coupons thus results are here omitted. Further details are given in the conclusions.
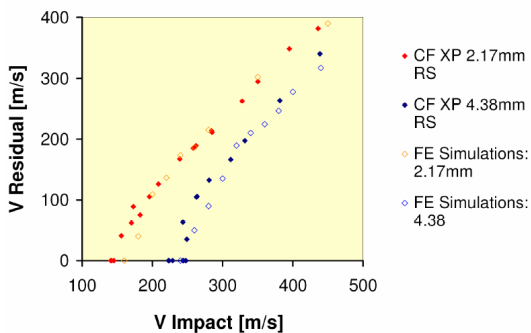

Fig. 16. Ballistic tests data and numerical results: effects of target thickness.
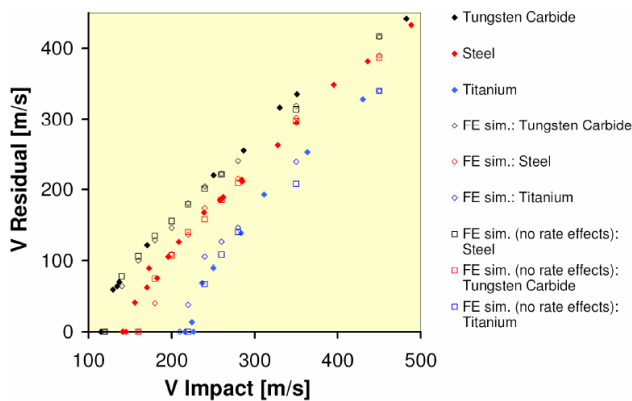

Fig. 17. Ballistic tests data and numerical results: effects of projectile density.
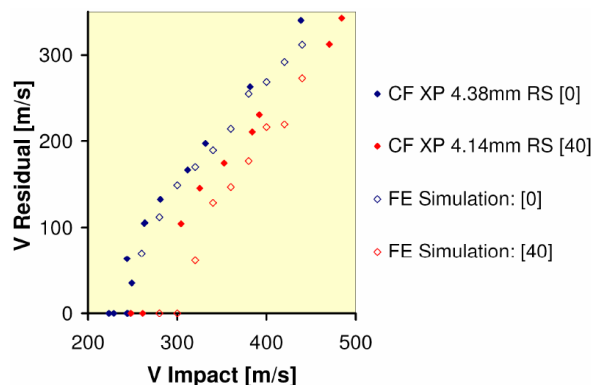

Fig. 18. Ballistic tests data and numerical results for CF XP 4mm coupons impacted by a 6mm-diameter steel ball at 40° incidence.
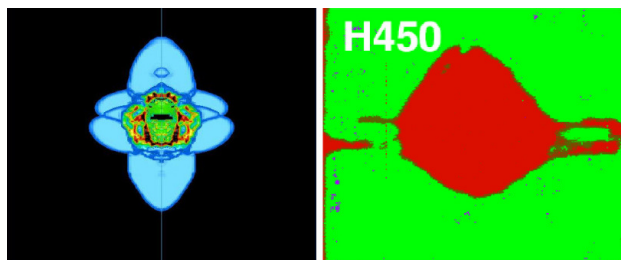

Fig. 19. Comparison of numerical (left) and experimental (right) impact damage areas for an impact at 260m/s at 40° incidence.

4 Conclusions

In the present investigation, high velocity impact tests were performed on CF NCF/RTM6 composite specimens using a gas gun apparatus. The effects of varying projectile density, impact angle,

8

impact velocity, target thickness and lay-up were investigated.

This paper has also described the formulation of an original numerical composite material model suitable for predicting the high velocity impact behaviour of polymer composites made with UD carbon fibrous reinforcement. The model is based on the combined application of: a) an original physical based formulation for modelling the non-linear strain-rate dependent response of the polymer matrix and its effects on composites behaviour under dynamic loading; b) Physically based dynamic criteria for matrix compressive and tensile damage initiation, simple maximum dynamic stress failure criteria for pure shear failure, and static failure criteria for fibre tensile and compressive failure; c) An original strain rate-dependent damage mechanics approach based on fracture mechanics.

The model has been successfully implemented in the FE explicit code LS-DYNA3D. It was applied at predicting the response of NCF/RTM6 coupons for varying impact conditions and target parameters including target thickness, lay-up of the target laminate, impact angle and projectile density. The numerical results from over 70 simulations were reduced in the form of ballistic curves. A series of conclusions can be drawn:

- A good correlation is obtained between the numerical and the experimental ballistic curves for varying target thickness, impact angle, projectile material and target lay-up.

- The energy absorbed through ballistic penetration does not appear to be affected by strain-rate effects (Fig. 20), but the use of a strain-rate dependent failure and damage formulation can improve the correlation between numerical and experimental damage areas, especially for higher impact velocities.

- The correlation between the numerical and the experimental matrix damage area is however not always satisfactory. The experimental damage area is under-estimated by the model and this is found more evident for thicker specimens. This can be explained as the smeared formulation here applied cannot predict fibres splitting thus lifting mechanism played by split and broken fibres of the inner layers on the rear-face ply of the target upon projectile penetration. The rear-face ply undergoes the most severe delamination compared to all other plies in the specimen.

- Further numerical simulations could use interface elements [23, 24]. The formulations proposed in refs. [23, 24] could be easily modified including

strain-rate-dependent damage evolution laws as those that were proposed in the present paper. The formulation proposed here for the modelling of strain-rate dependent damage propagation law is judged flexible enough to allow for the dynamic scaling functions to be determined with an inverse approach. This could be done by means of a parametric analysis based on iterative comparison between the numerical and experimental damage areas. Such a research would lead to a greater understanding of the influence of strain rate on damage propagation.

- The results are strongly dependent on the strategy adopted for element erosion. Eroding greatly distorted elements is, however, a necessity when modelling ballistic penetration with Lagrangian FE techniques. A strategy for element erosion has been established based on the use of a maximum shear strain erosion parameter. Further impact tests and numerical simulations should be conducted for different (fully characterised) composite material systems in order to confirm whether or not the value of the erosion parameter depends on physical and mechanical properties of the target. A good correlation was obtained for the variation of the debris mass with varying impact energy [19], which supports the chosen value for the erosion parameter.

- Meshless methods, such as SPH or partition of unity methods, which do not require a strategy for element erosion, would improve the performances of energy based damage models in which failure is predicted by the application of "directional" (or "modal") failure criteria.

- The energy-based damage mechanics approach used in the current model ensures objectivity of the solution with mesh refinement. However, the current formulation can handle structured mesh only. The implementation, in the current formulation, of an objectivity algorithm which can handle non-structured mesh, e.g. [25], is suggested for future developments of the material model discussed in this paper.

- Experimental work should be conducted for characterisation of the dynamic fracture toughness of the composite in the failure modes predicted by the failure criteria that were applied.

- Strain-rate-dependent constitutive laws for the fibre direction should be formulated and implemented for the modelling of the dynamic behaviour of glass fibrous composites, which are remarkably strain-rate sensitive in this direction.

References

[1] Bibo, G.A., P.J. Hogg, R. Backhouse and A. Mills. "Carbon-fibre non-crimp fabric laminates for cost-effective damage-tolerant structures". *Composites Science and Technology*, Vol. 58(1), pp. 129-143, 1998.

[2] Breen, C.E.P., F.J. Guild and M.J. Pavier. "Thick NCF Composite Laminates: Low Velocity Impact Performance". *Proceedings of 15th International Conference on Composite Materials - ICCM-15*, Durban, South Africa, pp. 155-156, 1998.

[3] Larsson, F. and L. Svensson."Carbon, polyethylene and PBO hybrid fibre composites for structural lightweight armour". *Composites Part A*, Vol. 33(2): pp. 221-231, 2002.

[4] Lopresto, V., G. Caprino and A. Busco. "Effect of blanket manufacturing variables on the impact behaviour of non-crimp fabric laminates". *Proceedings of Composites Europe 2005*, Barcelona, Spain, paper no. 154, 2005.

[5] Wonderly, C., J. Grenestedt, G. Fernlund and E. Cepus. "Comparison of mechanical properties of glass fiber/vinyl ester and carbon fiber/vinyl ester composites". *Composites Part B*, Vol. 36(5), pp. 417-426, 2005.

[6] Raimondo, L., L. Iannucci, P. Robinson, J. Hodgkinson, P.T. Curtis and G.M. Wells. "Developments in vacuum assisted resin infusion for cost-effective manufacture of composite panels, with emphasis on surface finish quality". *Submitted to Composites Part A*, 2006.

[7] *Advanced composite compression tests. Boeing specification support standard*. BSS 7260, 1986.

[8] Raimondo, L., L. Iannucci and P. Robinson. "*The impact behaviour of NCF reinforced epoxy composite*". TR01/07, The Composite Centre, Imperial College London, UK, 2007.

[9] Davies, G.A.O. and E.W. Godwin. "Impact beahviour of thermoplastic composite". *CADCOMP*. Springer Verlag: New York. pp. 371-382, 1988.

[10] Iannucci, L. and J. Ankersen. "An energy based damage model for thin laminated composites". *Composites Science and Technology*, Vol. 66(7-8), pp. 934-951, 2006.

[11] Allix, O. "A composite damage meso-model for impact problems". *Composites Science and Technology*, Vol. 61(15), pp. 2193-2205, 2001.

[12] Chen, J.K., F.A. Allahdadi and T.C. Carney. "High-velocity impact of graphite/epoxy composite laminates". *Composites Science and Technology,* Vol. 57(9-10), pp. 1369-1379, 1997..

[13] Cheng, W.L., S. Langlie and S. Itoh. "High velocity impact of thick composites". *International Journal of Impact Engineering*, Vol. 29(1-10), pp. 167-184, 2003.

[14] Riedel, W., W. Harwick, D.M. White and R.A. Clegg. *"ADAMMO – Advanced Material Damage Models for Numerical Simulation Codes. Final Report"*. EMI: Freiburg, 2003.

[15] Pinho, S.T., L. Iannucci and P. Robinson. "Physically-based failure models and criteria for laminated fibre-reinforced composites with emphasis on fibre kinking: Part II: FE implementation". *Composites Part A*. Vol. 37, pp. 766-777, 2006.

[16] Donadon, M.V. "*The structural behaviour of composite laminates manufactured using resin infusion under flexible tooling"*, PhD thesis, Department of Aeronautics. Imperial College London, UK, 2005.

[17] Pinho, S.T. "Modelling failure of laminated composites using physically-based failure models", PhD thesis, Department of Aeronautics. Imperial College London London, UK, 2005.

[18] Pinho, S.T., L. Iannucci and P. Robinson. "Physically-based failure models and criteria for laminated fibre-reinforced composites with emphasis on fibre kinking: Part I: Development". *Composites Part A*, Vol. 37(1), pp. 63-73, 2006..

[19] Raimondo, L. "*Predicting the dynamic behaviour of polymer composites"*, PhD thesis, Department of Aeronautics. Imperial College London, UK, 2007.

[20] van Paepegem, W., I. de Baere and J. Degrieck. "Modelling the nonlinear shear stress-strain response of glass fibre-reinforced composites. Part I: Experimental results". *Composites Science and Technology*, Vol. 66, pp. 1455-1464, 2006.

[21] Hsiao, H.M., I.M. Daniel and R.D. Cordes. "Dynamic Compressive Behavior of Thick Composite Materials". *Experimental Mechanics*, Vol. 38(3), pp. 172-180, 1998.

[22] Hallquist, J.O. "*LS-DYNA Theorethical Manual, version 970*", 1998.

[23] Pinho, S.T., L. Iannucci and P. Robinson. "Formulation and implementation of decohesion elements in an explicit finite element code". *Composites Part A*, Vol. 37(5), pp. 778-789, 2006.

[24] Iannucci, L. "Dynamic delamination modelling using interface elements". *Computers and Structures*, Vol. 84(15-16), pp. 1029-1048, 2006..

[25] Oliver, J. "A consistent characteristic length for smeared cracking model". *International Journal for Numerical Methods in Engineering*. Vol. 28, pp. 461-474, 1989.